


RESEARCH

Open Access



# Analyzing the potential of full duplex in 5G ultra-dense small cell networks

Marta Gatnau Sarret<sup>1\*</sup> , Gilberto Berardinelli<sup>1</sup>, Nurul H. Mahmood<sup>1</sup>, Marko Fleischer<sup>2</sup>, Preben Mogensen<sup>1,3</sup> and Helmut Heinz<sup>2</sup>

## Abstract

Full-duplex technology has become an attractive solution for future 5th generation (5G) systems for accommodating the exponentially growing mobile traffic demand. Full duplex allows a node to transmit and receive simultaneously in the same frequency band, thus, theoretically, doubling the system throughput over conventional half-duplex systems. A key limitation in building a feasible full-duplex node is the self-interference, i.e., the interference generated by the transmitted signal to the desired signal received on the same node. This constraint has been overcome given the recent advances in the self-interference cancellation technology. However, there are other limitations in achieving the theoretical full-duplex gain: residual self-interference, traffic constraints, and inter-cell and intra-cell interference. The contribution of this article is twofold. Firstly, achievable levels of self-interference cancellation are demonstrated using our own developed test bed. Secondly, a detailed evaluation of full-duplex communication in 5G ultra-dense small cell networks via system level simulations is provided. The results are presented in terms of throughput and delay. Two types of full duplex are studied: when both the station and the user equipments are full duplex capable and when only the base station is able to exploit simultaneous transmission and reception. The impact of the traffic profile and the inter-cell and intra-cell interferences is addressed, individually and jointly. Results show that the increased interference that simultaneous transmission and reception causes is one of the main limiting factors in achieving the promised full-duplex throughput gain, while large traffic asymmetries between downlink and uplink further compromise such gain.

**Keywords:** Full duplex, 5G, Small cell, Throughput, Delay, Interference, Traffic profile

## 1 Introduction

Wireless communication is stimulating a networked society, where data is exchanged anytime, everywhere, between everyone, and everything. In 2000, only 10 GB of mobile data traffic was reached per month, whereas in 2015 such amount represented 3.7 billions of gigabytes [1]. This enormous traffic increase was generated by several causes: the introduction of new services and applications, the massive use of social networks, and the utilization of smart devices with mobile data connection, such as smartphones and phablets, among others. The amount of carried data will continue to grow, and it is expected to be eightfold in 2020, with reference to 2015. A new 5th generation (5G) radio access technology

is expected to accommodate the exponentially growing demand of mobile traffic. Several strategies may be considered for boosting capacity, such as cell densification or multiple-input multiple-output (MIMO) technology with a large number of antennas. Recent advances in transceiver design have also attracted the attention of the research community on full-duplex (FD) technology. FD allows a device to transmit and receive simultaneously in the same frequency band, thus, theoretically, doubling the throughput over traditional half-duplex (HD) systems. Given the capabilities of this technology, it is considered as a potential candidate for future 5G systems.

A 5G concept tailored for small cells was proposed in [2], optimized for dense local area deployments. The system assumes the usage of  $4 \times 4$  MIMO transceivers and receivers with interference suppression capabilities. Though originally designed as a HD time division duplex

\*Correspondence: mgs@es.aau.dk

<sup>1</sup>Department of Electronics Systems, Aalborg University, Fredrik Bajers Vej 7, 9220 Aalborg, Denmark

Full list of author information is available at the end of the article

(TDD) system, the proposed concept can easily support FD communication. In order to have an operational FD node, the self-interference (SI), i.e., the interference caused by the transmit antenna to the receive antenna located in the same device should be attenuated as much as possible, ideally below the receiver noise power level. Several techniques were proposed to provide high levels of self-interference cancellation (SIC) [3–7]. In [7], a detailed study of the passive SIC for FD infrastructure nodes is presented. Several techniques are analyzed, individually and jointly, and then evaluated experimentally. The authors argue that the main problem in SIC are the reflections or multi-path, while the direct link is easier to cancel. The former requires active suppression while the latter is tackled with passive cancellation. For this reason, the authors recommend to apply both active and passive cancellations whenever possible. Finally, the experimental results show that the most appropriate approach is to combine directional antennas with cross-polarization and an absorber. Recent results show that SI can be reduced of around 100 dB [6, 8]. This may suffice for considering FD a realistic option, at least according to transmit power constraints.

The promised FD throughput gain may be compromised by several limitations. First, the residual SI may still negatively affect the reception of the desired signals. In addition, the increased interference caused by FD and the traffic profile may further compromise such theoretical FD gain. FD doubles the amount of interfering streams, leading to an increased inter-cell interference (ICI). Furthermore, exploiting FD is only possible when there is data traffic in both link directions, uplink (UL) and downlink (DL).

There are three kinds of FD applications. The first is the relay FD, where the base station (BS) is FD capable and relays data from HD user equipments (UEs). Relay FD is thoroughly analyzed in [9] for two use cases, amplify-and-forward (AF) and decode-and-forward (DF). The available self-interference cancellation techniques are also intensively described. An interesting outcome of [9] is that the biggest beneficiaries of FD might be the networks that have short communication range and low transmit power, such as small cells. Furthermore, in [10], the impact of non-ideal SIC on the end-to-end network capacity is analyzed in the context of FD relaying. The authors propose a power allocation scheme to reduce the SI. The results show gains close to the theoretical double throughput. However, the authors do not consider either the impact of inter-cell interference or the traffic profile. The work presented in this article focuses on the other two types of FD: the case where both the BS and the UE are FD capable, namely bidirectional FD, and the BS FD configuration, which refers to the situation where only the BS is able to exploit simultaneous transmission and reception with

HD users. Consequently, the literature presented next will focus on these two cases.

A novel design of a FD MIMO radio is presented in [11]. The authors' proposal provides meaningful results on SIC, reducing the complexity, cost and error of current models. However, the evaluation of the FD gain is extracted under unrealistic conditions, i.e., without considering the impact of the inter-cell interference and the traffic profile.

A number of studies analyzes the FD performance in small cell scenarios [12–18] and in a macro cell network [19] based on interference levels, disregarding the type of traffic in the network. In [12], the gain that FD provides compared to HD, assuming ideal SIC, is analyzed from a signal-to-interference-plus-noise ratio (SINR) perspective. The authors conclude that the FD gain is below the promised 100%. The authors in [13, 14] study the achievable bit rate depending on different residual SIC levels and interference conditions. Both works analyze the SINR region where FD outperforms HD, concluding that in highly interfered scenarios, switching between FD and HD provides the optimal results. In [15], the FD throughput performance using different types of receivers and ideal SIC in a multi-cell scenario is studied. Results show an average throughput gain of 30–40%. In [16], results comparing MIMO HD and FD are presented, assuming full buffer traffic. The authors conclude that, without interference, FD can provide up to 31 and 36% gain in terms of throughput and delay, respectively, while in case of interfered scenarios, HD may outperform FD due to MIMO spatial multiplexing gains. Tong and Haenggi [17] focus on an ALOHA system to provide analytical expression to optimize the capacity given the density of FD and HD nodes. The region where FD outperforms HD is studied, under the assumption of non-ideal SIC, but without considering the impact of the traffic profile. The authors conclude that achieving the double throughput gain is not possible, and the FD gain depends on the level of SIC. The impact of user-to-user or intra-cell interference is studied in [18]. The authors demonstrate via simulation results that setting a different transmit power for the BS and UE has a positive impact on the network performance, even under residual SI. A power control algorithm to maximize the sum rate of DL and UL via an efficient switching between HD and FD is proposed in [19]. The authors show that there is a SINR region where HD outperforms FD.

The impact of the traffic type is addressed in the studies [6, 8, 20–23]. Goyal et al. [20] propose a hybrid FD/HD scheduler that selects the mode that maximizes the network throughput. The evaluation is carried out considering asymmetric traffic, showing that FD always outperforms HD. However, a strong isolation between the

cells is assumed, which may downgrade the ICI impact. Malik et al. propose a power control algorithm to accommodate asymmetric traffic [21]. The proposed scheme, evaluated in a single cell scenario, shows an improvement in DL at the expense of lowering the UL rate. Mahmood et al. [22] study the impact of symmetric and asymmetric traffic in a multi-cell scenario. Throughput results show that the FD gain reduces with the perceived ICI and the traffic ratio. Heino et al. [6] conclude that in dense deployment of small cells, where transmit powers are low and distances among nodes are short, 100 dB of SIC is sufficient to consider ICI as the main limiting factor for achieving the promised FD gain. Moreover, they remark that large asymmetric traffic ratios between DL and UL data may compromise the usage of FD and hence its gain. These challenges are also described in [8, 23].

The above-mentioned works study the performance of FD assuming User Data Protocol (UDP) traffic. However, most of the Internet traffic is carried over Transport Control Protocol (TCP) flows, with a small percentage of UDP flows [24]. TCP [25] is used to provide a reliable communication and reduce packet losses. Its congestion control mechanism limits the amount of data that can be pushed into the network, based on the reception of positive acknowledgments (ACKs) [26]. This procedure causes an increase in the delay and a reduction of the system throughput. FD may mitigate such drawbacks since it may allow to accelerate the TCP congestion control mechanism, given the possibility of transmitting and receiving simultaneously. It is important to notice that the previously mentioned works disregard the usage of features such as link adaptation and recovery and congestion control mechanisms.

In this paper, we perform a system level evaluation of the full-duplex performance in dense small cells, where the impact of the traffic profile and the inter-cell and intra-cell interferences is addressed, individually and jointly. The study is carried using a system level simulator which implements both the lower and the upper layers of the Open Systems Interconnection (OSI) model and features mechanisms such as link adaptation and recovery and congestion control mechanisms. The contribution of this paper is twofold. Firstly, achievable levels of SIC are demonstrated using our own developed test bed. Secondly, a detailed evaluation of FD communication in 5G ultra-dense small cell networks is provided. Two types of FD communication are studied: BS FD and bidirectional FD. We consider the cases where the traffic is symmetric in DL and UL and when the offered load between both links is asymmetric. Furthermore, the analysis of the traffic constraints is provided with both TCP and UDP traffic. The results are presented in terms of throughput and delay and they show that the increased

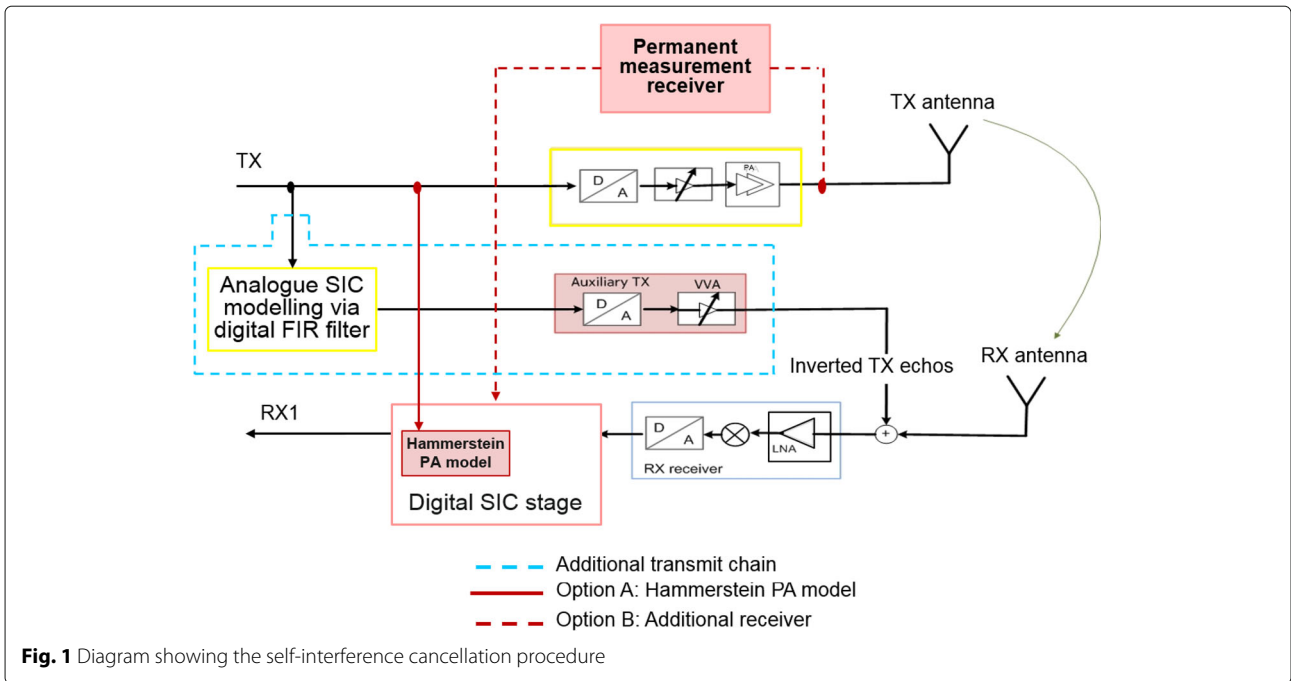
interference that simultaneous transmission and reception causes is one of the main limiting factors in achieving the promised full-duplex throughput gain. Large traffic asymmetries between DL and UL further compromise such gain. Nevertheless, FD shows potential in asymmetric traffic applications where the lightly loaded needs to be improved, both in terms of throughput and delay.

The structure of the paper is as follows: Section 2 presents our own developed test bed and the most recent results; Section 3 describes the envisioned 5G system featuring FD communication; Section 4 introduces the simulation environment, including the simulation tool and the simulation setup; Section 5 discusses the results; Section 6 describes the future work; finally, Section 7 concludes the paper.

## 2 Self-interference cancellation

A FD node generates a self-interference signal power that could easily exceed the power of the desired signal by 100 dB or more [6]. For this reason, providing a high level of SIC is a fundamental requirement to build an operational FD node. In order to identify the potential limits of SIC, we have developed a demonstrator system at Nokia Solutions and Networks in Ulm. The concept proposed in [27] and depicted in Fig. 1 has been build and studied. Such concept consists of a pre-mixer with an additional transmit chain for analogue compensation and a final digital cancellation stage. Up to 100-MHz contiguous bandwidth can be handled by the system, which is typically operating in the 2.4-GHz band. The practical antenna isolation from the transmitter (TX) to the receiver (RX) is  $\sim 50$  dB and is based on physical antenna separation, as shown in Fig. 2, and the appropriate passive means. Additionally, to limit the impact of the phase noise, it is essential to provide a common clocking domain, same mixer stage for up and down conversion, and radio frequency (RF) delay compensation [28].

The used hardware has the capability of canceling maximum  $\sim 70$  dB for a 20-MHz LTE signal (LTE20) with respect to phase noise. The achievable active cancellation is limited by the power amplifier (PA) non-linearity and the auxiliary transmitter resolution. Under these two limitations, a total active cancellation gain of 63 dB for a LTE20 signal could be demonstrated, with a joint usage of the analogue cancellation and the time domain digital cancellation stages. There are two approaches to achieve such gain. The first one is the option A depicted in Fig. 1 that uses a non-linear intermodulation approach via Hammerstein PA model [29] within the digital SIC stage. This option employs the digital transmit signal as input [30]. The second approach, plotted as the option B in Fig. 1, uses the PA signal as direct input to the digital SIC

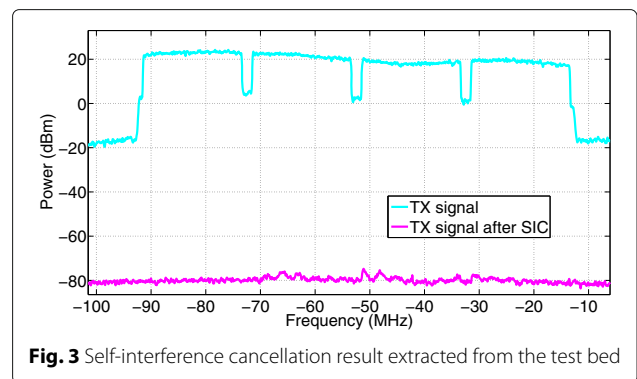
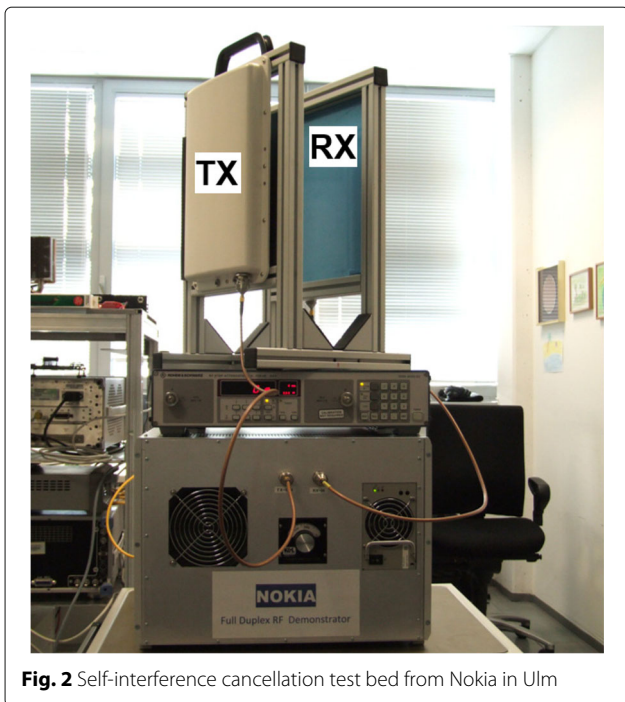


stage with the need of an additional receiver, named the *permanent measurement receiver*, which contains the transmitter RF impairments and is common in a typical commercial RF design for PA linearization purposes.

The design shown in Fig. 1 also requires the usage of an additional transmit chain. Such additional transmit block

has the purpose to protect the receiver against saturation, and it has the advantage that scales only with the number of transmit antennas, which is highly appropriate in MIMO systems. Furthermore, to avoid extra complexity and provide simpler hardware integration, all transmitted antenna streams are input to the same analogue and digital SIC modeling block.

A total cancellation of  $\sim 100$  dB for a 20 dBm  $4 \times$  LTE20 signal has been demonstrated, as shown in Fig. 3. The result shows the SI level close to receiver noise floor limits ( $-85$  dBm, considering a noise figure of 10 dB), thus demonstrating the potential of the described hardware concept. Achieving a large level of SIC at higher frequencies beyond today's LTE limits, wider frequency bands of hundreds of MHz, and large number of antennas is still an open research topic.



### 3 Full duplex in 5G small cells

#### 3.1 Featured 5G system design

Since the goal of this work is to study FD in dense small cell networks considering system level aspects, in this section, we are going to describe the small cell concept which will be the reference for our evaluation.

The small cells concept presented in [2] was originally designed as a HD TDD system with orthogonal frequency division multiplexing (OFDM) as modulation scheme, but it can easily accommodate FD communication. Nodes are assumed to be synchronized in time and frequency and equipped with  $4 \times 4$  MIMO transceivers with interference rejection combining (IRC) capability [31]. A novel frame structure of duration 0.25 ms is introduced, which is defined as the transmission time interval (TTI) and is shown in Fig. 4. The first two OFDM symbols are dedicated to the DL and UL control, respectively. The remaining symbols are allocated for the data, including the demodulation reference signal (DMRS) symbol, which is used for channel estimation. The IRC receiver requires information about the channel responses of the desired and the interfering signals to provide a good performance. Such channel information can be obtained by relying on orthogonal reference sequences transmitted by multiple devices in the DMRS symbol. Then, exploiting such information, it suppresses a number of the interfering streams according to the available degrees of freedom in the antenna domain [31]. Furthermore, recovery mechanisms such as hybrid automatic repeat and request (HARQ) and automatic repeat and request (ARQ) are used to deal with the residual ICI. For further details regarding the system design, the reader should please refer to [2, 32].

Using the same frame structure for both UL and DL allows for a straightforward extension of the envisioned 5G concept to FD transmission. Note that the control part remains as HD, in order to support different types of FD communication. The cell operations are as follows: firstly, the BS sends the scheduling grant (SG) in the DL control symbol of  $TTI_n$ . The SG includes the scheduled UE and the transmission parameters, i.e., the direction (UL or DL), the modulation and coding scheme (MCS) and the number of spatial streams used for transmission, often referred as transmission *rank*. The configuration specified in the SG is applied in  $TTI_{n+1}$

assuming a certain processing time. Consequently, there is one TTI delay between the scheduling and the corresponding data transmission. The UEs send the scheduling request (SR) in the UL symbol, including buffer information, HARQ feedback and the MCS and rank derived from their channel measurements. Notice that there is a delay between the instant when the channel is measured and the TTI when the transmission occurs, which may affect the link adaptation procedure. In addition, since the transmission direction may change at each TTI, creating sudden changes in the interference pattern, it further compromises the link adaptation procedure.

In this study, two FD techniques are investigated, which are depicted in Fig. 5. In the figure, full lines represent the intended transmissions and dashed lines refer to interfering streams. Figure 5a shows the bidirectional FD case, where both the BS and the UEs are FD capable. In this case, the communication is performed always between the same pair BS-UE, and therefore both nodes only perceive their own SI. The second FD mode is the BS FD, shown in Fig. 5b, where only the BS is FD capable. In this case, the DL and UL scheduled UEs are different. Therefore, the intra-cell interference, i.e., the interference from the UL UE to the DL UE, also affects the system performance. Notice that in case of a multi-cell scenario, the ICI would affect the performance of the system.

When FD is exploited, the number of interfering streams compared to HD is doubled. Therefore, the network interference is larger in FD than in HD, and the performance of the IRC receiver may be jeopardized since it may not have enough degrees of freedom in the antenna domain to deal with the enlarged interference. On the other hand, FD transmission will be only exploited in case there is data available at both BS and UE. Hence, the theoretical gain that FD can provide over HD may be compromised by the following limitations:

- Residual self-interference. For a FD node to be operational, a high level of isolation between the transmitting antenna and the receiving antenna located in the same device is required. Current levels of achievable SIC may not sufficient to bring the SI power below the receiver noise power level, thus leaving a residual interference that affects the SINR.

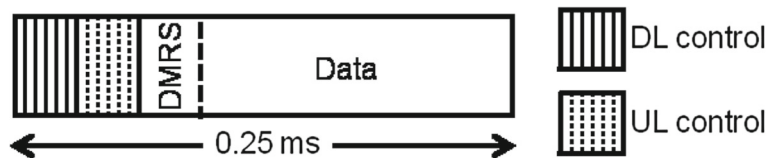
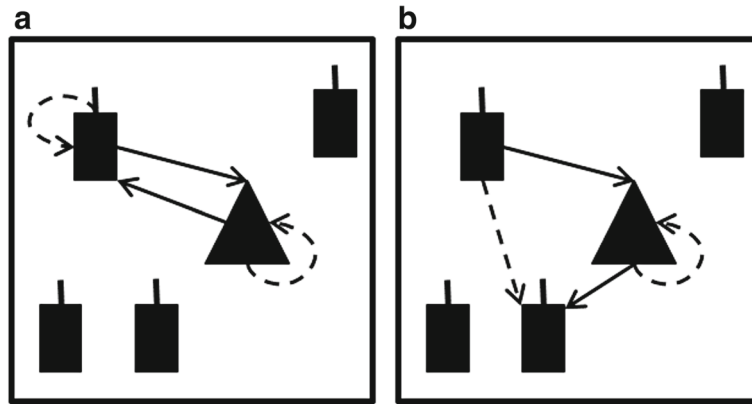


Fig. 4 Envisioned 5G frame structure



**Fig. 5** Full-duplex types. The *dashed lines* represent interference and the full lines the desired signal. **a** Bidirectional FD. **b** Base station FD

- Increased interference. The number of interfering streams with FD are doubled compared to HD, thus leading to an increased network interference (inter-cell and intra-cell interferences). Then, when the interference is stronger, the data rates are lower and consequently a larger number of TTIs is needed to transmit the same amount of data.
- Simultaneous UL and DL data. The availability of simultaneous UL and DL traffic dictates the probability of exploiting FD. Hence, large asymmetries between UL and DL may jeopardize the FD gain.

### 3.2 Radio resource management architecture

In order to support FD communication, a design for the radio resource management (RRM) module, shown in Fig. 6, is proposed. The RRM module decides which transmission mode is going to be used at each TTI (HD or FD), the transmission direction in case of HD, and which is(are) the node(s) that is(are) going to be scheduled. The module is divided into two blocks to reduce the complexity and the computational time. As the first step, the *direction decision block* decides the optimal transmission direction per each UE. This decision is extracted based on the information received from the physical (PHY), medium access control (MAC), and radio link control (RLC) layers. Such information includes SINR measurements, HARQ feedback, buffer status reports, and link quality information

provided by each UE to the BS. The set of decisions for all UEs extracted from the *direction decision block* is sent to the *user decision block*. Then, as the second step, the transmission mode (HD or FD) and the UE(s) to be scheduled will be decided by the *direction decision block*.

The optimal transmission direction, determined by the *direction decision block*, can be *DL*, *UL*, *DL+UL*, or *MUTE*, and it is extracted differently depending on the type of communication:

- *HD and BS FD*: for these two cases, the procedure to extract the optimal link direction is the same. In BS FD, a UE cannot be scheduled in both links because it operates in HD transmission mode. The transmission direction is decided based on the offered load of each link, and thus the amount of dedicated resources is proportional to the offered load. For example, let us assume asymmetric traffic, where the highly loaded link (DL) offers  $k$  times more load than the lightly loaded link (UL). In this case, the DL would get, in average,  $k$  times more resources than the UL, and it would have higher priority. Consequently, the UL would have to wait longer to be scheduled. Furthermore, the algorithm also takes into account fairness, by granting a minimum amount of resources to a link, in order to avoid its starvation. For more details about the used scheme, the reader should refer to [33]. The possible output directions in this

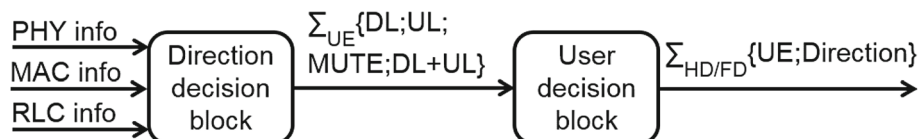


**Fig. 6** RRM module. The figure shows the design of the RRM module that supports both types of FD communication and HD

case are *DL*, *UL* or *MUTE*. The latter corresponds to the case where both UL and DL buffers are empty.

- *Bidirectional FD*: the transmission direction is based only on the buffer state. For each user, the *direction decision block* checks if there is data in both the DL and UL buffers. In case of bidirectional FD, simultaneous transmission and reception will only be exploited in case a UE can be scheduled in both links, which will happen only when both UL and DL buffers are filled with data. Then, if this is the case, the transmission direction for that user is *DL+UL*. Otherwise, it is *DL(UL)* if the UL(DL) buffer is empty and the DL(UL) is not, or *MUTE* if the UL and DL buffers are both empty.

In case of BS FD, a FD transmission is performed if two different UEs with opposite link directions can be scheduled; otherwise, the TTI is going to be HD. In case of bidirectional FD, it will be possible to exploit FD if at least one user has associated the *DL+UL* state. Note that in both cases, scheduling a FD transmission is always given priority over scheduling a HD one.

### 3.3 Interaction between full duplex and TCP

TCP [25] is a high layer protocol that aims at providing reliability by using a congestion control mechanism [26]. The amount of data that can be sent through the channel is limited based on the reception of positive acknowledgments (ACKs). The feature in charge of controlling such limitation is the congestion window, shown in Fig. 7. Within the *Slow Start* stage, the congestion window grows exponentially according to the received TCP ACKs. When the congestion window reaches the *Slow Start Threshold*, the *Congestion Avoidance* phase starts. In this stage, the growth of the congestion window is linear, following the same principle as the *Slow*

*Start* phase based on the reception of TCP ACKs. However, the TCP protocol has an inherent impact on the system throughput and delay because the amount of transmitted data is limited by the reception of ACKs, which will increase only if the channel conditions are favorable.

We believe that the TCP drawbacks may be mitigated by FD. Given the ability of simultaneous transmission and reception, the congestion window might grow faster and it might reach the *Congestion Avoidance* phase sooner, where a larger amount of data is transmitted within a single TTI. For clarification, an example of the congestion window growth for HD and FD in a single cell scenario with one AP and one UE is shown in Fig. 8. Both nodes have a 2-MB file to transmit and FD is exploited in all TTIs. In this example, shadowing and fast fading have been disabled to avoid the impact of the channel. The general simulation parameters are listed in Table 1, and they will be further discussed in Section 4. From the figure, we observe that FD transmits the 2-MB file faster than HD because the congestion window in case of FD is able to grow faster. In this example, the transmission time is reduced by nearly 45%.

## 4 Simulation environment

### 4.1 Simulation tool

The results presented in this study are extracted from our own developed event-driven based system level simulator, which layer structure is shown in Fig. 9. It includes the design of the envisioned 5G PHY and MAC layers presented in Section 2. The RLC, the TCP, and the UDP mechanisms are entirely modeled, whereas the Internet protocol (IP) is only modeled as overhead. In particular, the TCP version implemented in the simulator is New Reno [34], and it includes the recovery and congestion control mechanisms, whereas handshake procedures are not considered since they are not relevant for our studies. Two RLC modes are supported in the simulator, acknowledged (AM) and unacknowledged (UM). The former allows for packet reordering and packet

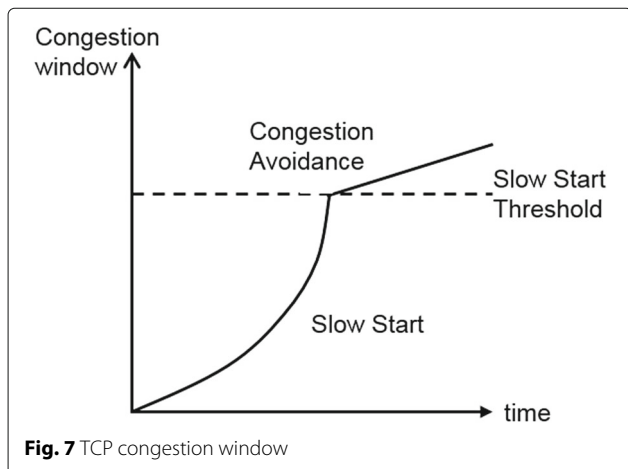


Fig. 7 TCP congestion window

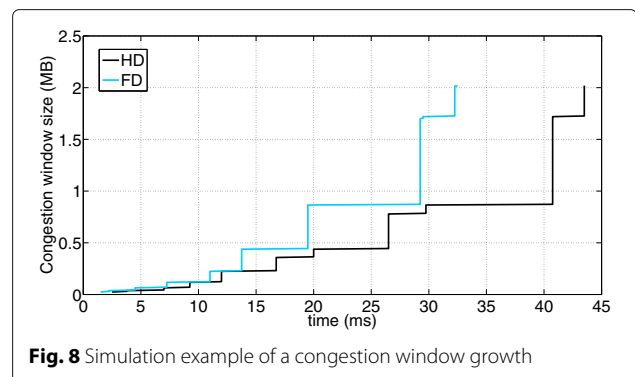
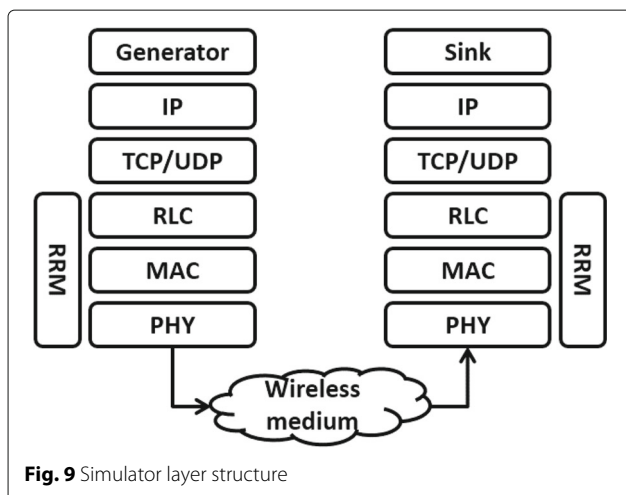


Fig. 8 Simulation example of a congestion window growth

**Table 1** Simulation parameters

Parameter	Value/state/type
System parameters	BW = 200 MHz; $f_c = 3.5$ GHz
Frequency reuse	1 (whole band)
Propagation model	WINNER II A1 w/fast fading [40]
Antenna configuration	4 × 4
Receiver type	IRC
Transmission power	10 dBm (BS and UE)
Link adaptation filter	Log average of five samples
Transmission rank scheme	Fixed or taxation-based
UL/DL decider	Metric (HD and BS FD) and traffic based (bidirectional FD)
HARQ max retransmissions	4
HARQ combining efficiency $\eta$	1
Resource utilization	~ 25, 50, and 75% if symmetric or asymmetric traffic 100% if full buffer traffic
RLC mode	Acknowledged
Transport protocol	UDP and TCP
Simulation time per drop	Up to 20 s
Number of simulation drops	50

retransmission in case of failure, which is controlled by sending positive acknowledgement packets (ACK) or negative acknowledgement packets (NACK). The latter only provides packet reordering, leaving the upper layers in charge of packet recovering. In case of AM, the acknowledgements are sent through the control channel, which means that they do not generate control overhead in the data plane. Therefore, the only retransmission mechanism that generates control overhead is TCP. A vertical RRM layer gathering information from the PHY, MAC, and RLC layers is implemented. The RRM layer includes the module described in Section 2 and decides



**Fig. 9** Simulator layer structure

the transmission parameters. The link adaptation feature extracts the most accurate MCS from the log-average of the last five SINR samples. The simulator supports 32 MCSs, extracted from a link level simulator and the lowest being Quadrature Phase Shift Keying (QPSK) with a coding rate of 1/5 and the highest being 256-Quadrature Amplitude Modulation (QAM) with a coding rate of 9/10. The MCS to SINR mapping is extracted according to a block error rate (BLER) target of 10%. The transmission rank can be either fixed or set dynamically according to a taxation-based rank adaptation algorithm [35]. Such algorithm runs in all nodes and decides the rank according to the perceived interference. The goal of the algorithm is to reduce the overall network interference level by applying a higher taxation to transmissions with higher ranks. The algorithm is further detailed in [35].

The channel model is Winner II A1 with fading. Such fading is extracted from a link level simulator, providing a channel coherence time of 10 ms. A transmitting node will decide how many antennas to use for transmitting different information (spatial multiplexing) over the whole bandwidth. At the receiver side, both desired and interfering streams arrive at the antennas and the IRC performs interference suppression based on the available degrees of freedom in the antenna domain. The SINR is calculated as follows:

$$\text{SINR} = \frac{P_T \cdot \alpha_d}{N + \sum_{i=1}^I P_T \cdot \alpha_i} \quad (1)$$

where  $P_T$  refers to the transmit power,  $\alpha_d$  is the pathloss between the transmitter and the intended receiver,  $N$  is the receiver noise power, and  $\alpha_i$  is the pathloss between the interfering nodes and the intended receiver.

The SINR extracted from this procedure is input to the decoding module. Such module decides whether the packet can be decoded or not. In case of failure, the HARQ mechanism will notify the RRM module that a retransmission is required. Note that the use of advanced receivers helps at resolving collisions by suppressing part of the incoming interference. On the other hand, if the packet is successfully decoded, it is sent to the higher layers up to the statistics module where the delay and throughput are computed. A SINR soft combining model extracts the effective SINR upon retransmissions. Soft combining keeps memory of previous transmissions of the same packet to achieve SINR gain and improve the probability of correct detection [36]. The model can be expressed as follows:

$$\text{SINR}_{\text{effective}} = \sum_{i=1}^n \text{SINR}_i \cdot \eta^{n-1} \quad (2)$$



where  $n$  refers to the transmission number,  $\text{SINR}_i$  is the SINR for the  $i$ th transmission/retransmission of the same packet, and  $\eta$  is the combining efficiency, used to model the non-ideality of the combining process. In this study, it is set to 1.0 for simplicity.

The simulator includes different traffic models, such as full buffer or File Transfer Protocol (FTP) [37]. The FTP traffic model generates payloads according to a negative exponential distribution. Such payloads, defined as sessions, have an average size of 2 MB and arrive every  $t_{\text{inter-arrival}}$  seconds. The parameter  $t_{\text{inter-arrival}}$  is also generated according to a negative exponential distribution. It is composed of the period of time when the application generates the packets for a particular session ( $t_{\text{on}}$ ) plus the amount of time when no packets are being generated ( $t_{\text{off}}$ ). The values of  $t_{\text{on}}$  and  $t_{\text{off}}$  reflect the load in the system. So, for a fixed  $t_{\text{on}}$ , increasing  $t_{\text{off}}$  will translate into a lower load in the system and vice versa. The carried system load dictates the network resource utilization (RU), i.e., the channel occupancy, defined as the following:

$$\text{RU} = \frac{\sum_{t=1}^T \text{TTI}_{t=\text{TX}}}{\sum_{t=1}^T \text{TTI}_{t=\text{TX}} + \sum_{t=1}^T \text{TTI}_{t=\text{MUTE}}} \quad (3)$$

where  $\text{TTI}_{t=\text{TX}}$  refers to a DL HD, UL HD, or FD transmission and  $\text{TTI}_{t=\text{MUTE}}$  refers to the case where there is no data to be transmitted in any of the two link directions. The upper limit in the summation  $T$  represents the total number of simulated TTIs. The RU is an indication of how saturated is the system. If the system is saturated, it would be translated into high level of interference and vice versa. For example, a RU of 50% means that half of the time the channel is free and a RU of 100% indicates that the channel is always busy.

Several key performance indicators (KPIs) can be extracted from the simulator: SINR, statistics on the MCS and transmission rank selection, FD probability, average session throughput (TP), packet delay, etc. The session TP is defined as the amount of time required to successfully transmit a session. Then, the average session TP is the mean of all the computed session TPs. The packet delay is the time between the creation of a packet at the

transmitter generator and its successful reception in the receiver sink, including the buffering time. Finally, the probability of exploiting FD is defined as the following

$$\text{Prob}\{\text{FD}\} = \frac{\sum_{t=1}^T \text{TTI}_{t=\text{FD}}}{\sum_{t=1}^T \text{TTI}_{t=\text{FD}} + \sum_{t=1}^T \text{TTI}_{t=\text{HD}}} \quad (4)$$

where  $\text{TTI}_{t=x}$  refers to the type of communication performed on a TTI. Then,  $t$  can be FD or HD.

## 4.2 Simulation setup

The performance of FD is evaluated in different scenarios. A single cell network is defined as a  $10 \times 10 \text{ m}^2$  room, containing one BS and four UEs randomly deployed. The UEs are always affiliated to the BS in the same cell (closed subscriber group). The multi-cell scenario refers to a  $10 \times 2$  grid of single cell networks, as shown in Fig. 10. Ideal SIC is considered, given the current SIC capabilities [6], the short distances among nodes and the low transmit power, which is set to 10 dBm for all the nodes. The RLC mode is set to Acknowledged (AM) [38]. The TCP parametrization and the remaining simulation parameters are listed in Table 1. Finally, the selected scheme for the *user decision block* is time domain round robin, so frequency multiplexing is not considered.

The performance of FD is compared against that of HD. We consider two types of FTP traffic, symmetric and asymmetric. Symmetric traffic refers to the case where the offered load is the same in DL and UL (1DL:1UL). On the other hand, asymmetric traffic case corresponds to the situation in which the offered load in DL is six times larger than in UL (6DL:1UL). Three loads are simulated: low, medium, and high, which refer to a RU of nearly 25, 50, and 75% under ideal conditions, respectively. The results are presented in three formats: as numerical tables; as the cumulative distribution function (CDF) of the average session throughput (TP) and the packet delay; and as bar plots showing the comparison between the HD and FD performance with TCP and UDP. The latter protocol acts as a transparent layer, sending all the received data to the upper layers, without performing error checking or congestion control [39]. Finally, the gain in percentage that FD provides over HD is calculated as follows:

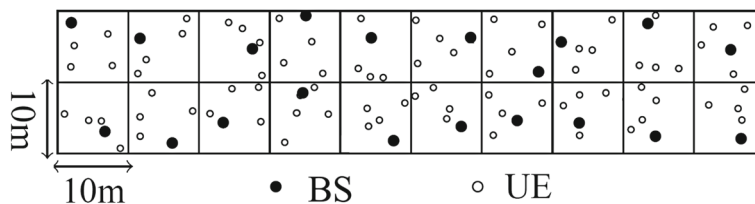


**Fig. 10** Multi-cell scenario. It corresponds to a grid of  $10 \times 2$  single cell networks

$$\text{Gain}_{\text{FD}}[\%] = \left( \frac{\text{FD average performance}}{\text{HD average performance}} - 1 \right) \cdot 100 \tag{5}$$

Such gain represents an increase in terms of throughput and a reduction in terms of delay; therefore for the first case, a gain will be indicated by the symbol “+” and in the second case it will be indicated by “-”.

### 5 Performance evaluation

The results provided in this section are presented in an order that aims at analyzing the impact of the increased interference caused by FD and the traffic constraints. In the first subsection, we focus on the analysis of the single cell network to avoid the impact of the inter-cell and intra-cell interference.

The multi-cell scenario will be analyzed in the second and third subsections. In first place, only the impact of ICI is quantified. For this reason, the bidirectional FD performance is analyzed by varying the penetration wall loss. Then, in the last subsection, the jointly effect of the ICI, the intra-cell interference (only for BS FD) and traffic constraints are evaluated.

#### 5.1 Analysis of the traffic constraint limitation

In this analysis, we analyze a single cell network with the transmission rank fixed to one. Bidirectional FD is considered. As a first step, the traffic generator is parametrized to generate symmetric traffic with a probability of having simultaneous traffic in UL and DL of 100%, i.e., FD can be exploited with 100% probability, and UDP is set as the transport layer. Figure 11 shows the average cell session TP and average packet delay. From the figure, we can observe that, under ideal interference conditions, the delay can be reduced by 50% and the TP can be increased by 93%, very close to the theoretical FD TP gain. This small difference in FD TP gain between the simulation results and the theoretical maximum is caused by the HD resource allocation algorithm used as a baseline, since it allocates the data optimally, as discussed in Section 2. The

FD gain would be 100% if the HD baseline is set to a fixed 1DL:1UL time slot allocation.

From this first result, we can conclude that it is possible to achieve the promised gain from FD but only under very specific conditions. The case of BS FD shows approximately the same performance (since the IRC receiver has sufficient degrees of freedom for suppressing the intra-stream interference given the usage of rank 1) and is not reported here. Let us evaluate the same scenario but in this case considering the low, medium, and high loads introduced in Section 4. Both the symmetric (1DL:1UL) and asymmetric (6DL:1UL) traffic cases will be addressed. Figure 12 shows the cell average session TP and the average packet delay for the symmetric traffic case. In such case, both link directions show approximately the same performance because the offered load is the same in UL and DL and interference is not present. The results show that FD always outperforms HD, and the gain that FD provides increases as the load grows. This gain increase is caused by a higher probability of exploiting FD.

Let us now consider TCP. The TCP protocol shapes the dynamics of the system by limiting the amount of data that can be sent by using a congestion control mechanism. Figure 13 shows the system performance (in terms of average cell session TP and average packet delay) with UDP and TCP, assuming symmetric traffic. The percentage numbers represent the gain that FD provides over HD. From the result, we can observe that the FD gain is larger when TCP is used. The reason is twofold: firstly, FD allows the TCP congestion window to grow faster, thus being able to transmit a larger amount of data than HD, as explained in Section 2; secondly, the probability of exploiting FD with TCP (from 85 up to 97%) is larger than with UDP (from 4 up to 37%). The FD probability is larger with TCP because data cannot be transmitted freely but under the constraints of the TCP congestion control mechanism, thus making the data accumulate in the buffer. In addition, since data is transmitted faster due to simultaneous transmission and reception, TCP ACKs have

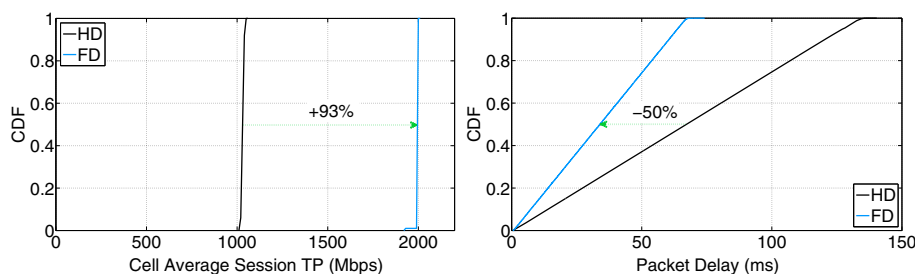
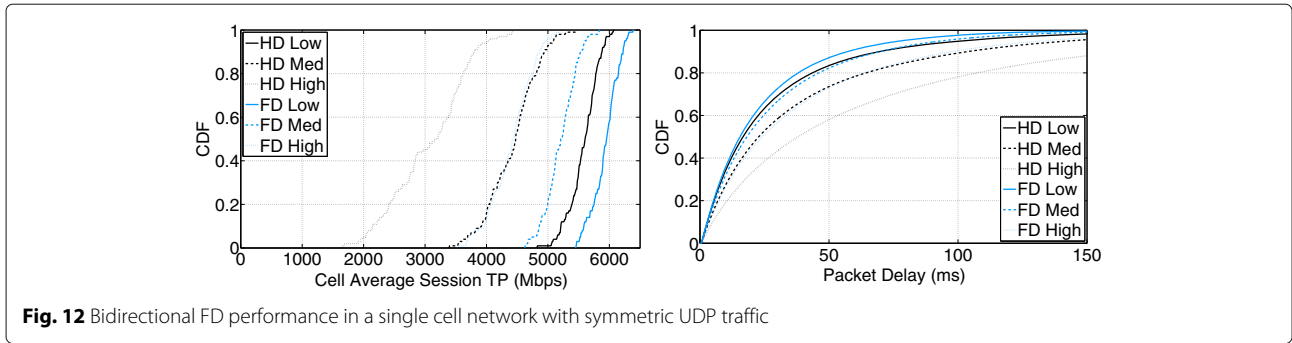


**Fig. 11** Bidirectional FD performance in a single cell network with 100% probability of exploiting FD



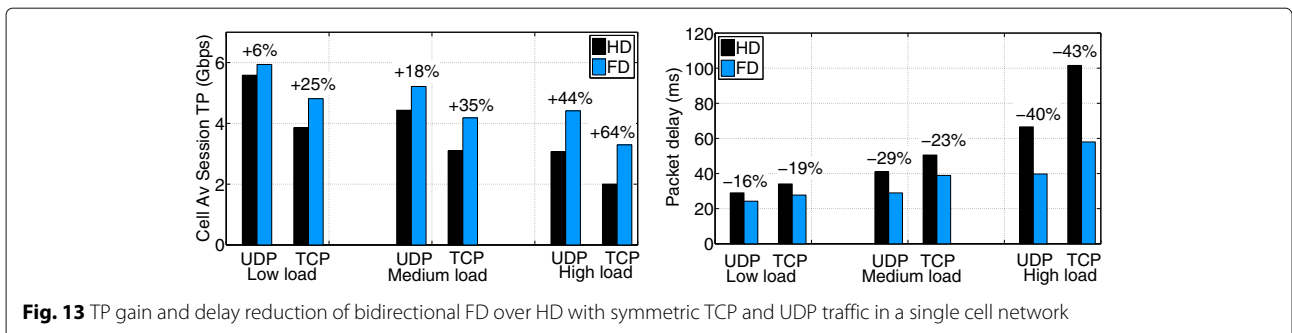
less chances of being piggybacked with data and hence are transmitted individually, like a normal data packet. So for example, in a single cell scenario, the number of non-piggybacked TCP ACKs with FD can be up to 2.7 times larger than with HD. Even though the TCP ACKs can be transmitted without delay with FD, they generate larger overhead if they cannot be piggybacked with data. Finally, it is important to notice that even if FD always outperforms HD in this specific scenario, the gain that FD provides is always below the theoretical one.

The asymmetric traffic case is shown in Fig. 14. Numerical results show the average session TP and packet delay in DL and UL separately and for both UDP and TCP. First of all, we can observe that, independently of the transport layer, the gain in UL and DL is now different. This is because in HD, according to the offered load of each link, six out of seven TTIs will be allocated to DL and one to UL, in average. In FD, since UL and DL can occur at the same time, DL can obtain, in average, one extra TTI compared to HD, while the UL can get six more. The results show the same trends as the symmetric traffic case: an increase of the FD gain for a larger offered load and a higher FD gain with TCP than with UDP. It is interesting to notice that in UL at high load, FD is able to eliminate the buffering or waiting time, being able to transmit all the data from the buffer. Furthermore, the DL data can be transmitted faster since the UL TCP ACK

can be transmitted immediately by exploiting FD communication. On the other hand, it generates a larger overhead due to not being able to piggyback it with data.

**5.2 Analysis of the inter-cell interference limitation**

To analyze how ICI affects the FD performance, we consider the multi-cell scenario shown in Fig. 10. The traffic model is now set to full buffer since we want to avoid the impact of the traffic constraints in the FD gain; the transport layer is UDP and the transmission rank is fixed to one for simplicity. The results are extracted by varying the penetration wall loss, which dictates the isolation between the cells, from 0 to 25 dB. In case the penetration wall loss is set to 0 dB, the simulated scenario would correspond to an open space network; while if it is set to 25 dB, it would refer to an almost isolated cell. The TP gain that FD provides over HD is depicted in Fig. 15. In the figure, the 5th, 50th, and 95th percentile gain are presented. The 5th percentile represents to the outage performance, i.e., the performance of the users perceiving the worst channel conditions. The results show that, as the isolation among cells increases, the gain that FD provides over HD increases. When the isolation among cells lowers, FD perceives larger ICI than HD because FD doubles the amount of interfering streams compared to HD. Notice that, even when the penetration wall loss is set to 0 dB, corresponding to the worst case, FD shows



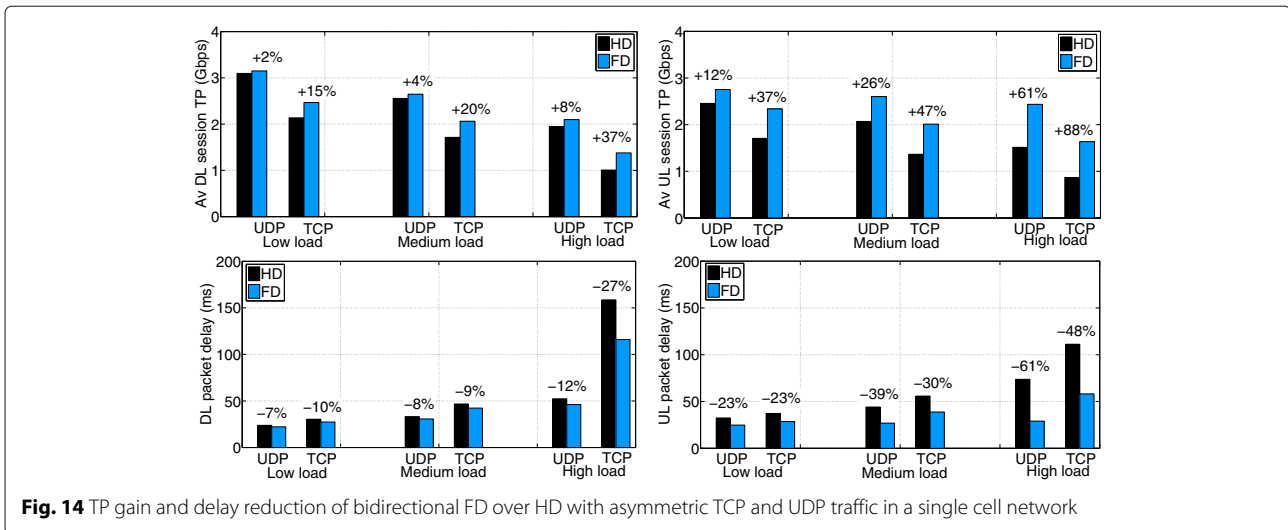


Fig. 14 TP gain and delay reduction of bidirectional FD over HD with asymmetric TCP and UDP traffic in a single cell network

an improvement of 9% over HD for the outage users. In addition, the 95th percentile, defining the users perceiving the best channel conditions, is improved by 56% with FD.

### 5.3 FD performance under the impact of increased interference and traffic constraints

In this last analysis, the joint impact of the increased interference caused by FD communication and the traffic constraints is analyzed. To that purpose, the multi-cell scenario with symmetric (1DL:1UL) and asymmetric (6DL:1UL) traffic and the rank adaptation algorithm described in Section 4 are used. The performance of HD and both types of FD communication with UDP and TCP for the medium load case (HD RU ≈ 50%) is presented.

Figure 16 shows the CDF of the DL and UL average session TP. Starting with the UDP performance, we observe that the UL and DL results with bidirectional FD are nearly the same. This is because the traffic is symmetric and thus both links would get the

same amount of resources, and the interference conditions perceived by all the nodes is in average the same. In this case, FD performs always better than HD, even showing an improvement of the outage users performance. However, for the BS FD case, the UL and DL directions show rather difference performance. The reason of such difference is the intra-cell interference. The DL user is highly interfered by the UL users. Therefore, the perceived interference conditions in the two links are different, and this affects the choice of MCS and transmission rank. Furthermore, the number of DL retransmissions is larger than in UL, creating an originally non-existing asymmetry in the traffic. This asymmetry causes the over-prioritization of the DL over the UL because the buffer size is larger, even though the offered load is the same. In this case, the DL is negatively impacted by the use of FD, since HD performs always better. The UL direction is barely optimized, showing that the outage users are negatively affected by the use of FD, while from the 50th percentile, FD outperforms HD. By analyzing the system behavior with TCP, we can observe that the results for the bidirectional FD communication are completely the opposite as the ones with UDP. The reason for this turnaround is the increased interference caused by a probability of exploiting FD of 81%, compared to 15% with UDP. Doubling the amount of interfering streams in almost every single TTI causes an average SINR difference of 9 dB between HD and FD, which has a repercussion on the MCS selection, the transmission rank and the link failures. HD is able to use a 12 times higher rate than FD, in average. Furthermore, the IRC receiver performance is jeopardized in case of FD given the increased interference, making the system limited to use rank 1, while HD is still able to switch to rank 2 sporadically.

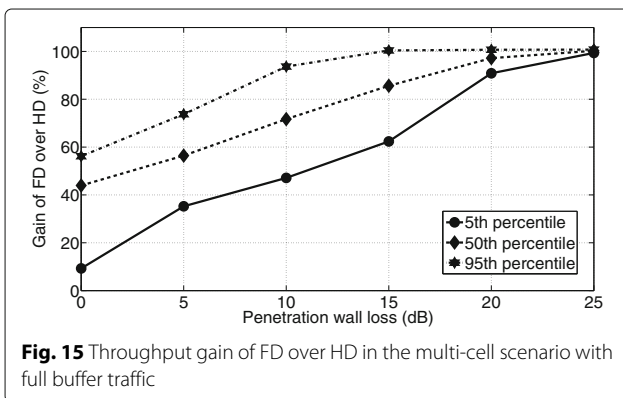
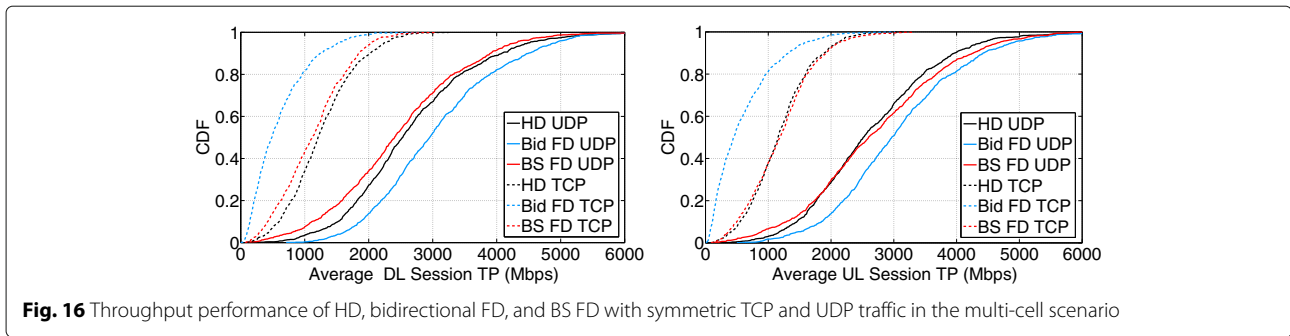


Fig. 15 Throughput gain of FD over HD in the multi-cell scenario with full buffer traffic



**Fig. 16** Throughput performance of HD, bidirectional FD, and BS FD with symmetric TCP and UDP traffic in the multi-cell scenario

Finally, the HARQ retransmissions are triggered more often with FD because the SINR reaches a level below the decodable threshold. For BS FD, the TCP trends are similar to the UDP ones because the probability of exploiting FD is nearly the same (25% in UDP and 32% in TCP). We can observe that the DL direction shows the best performance with HD, while the UL in this case is even closer than in the case of UDP. Notice that the RRM algorithm that decides the optimal transmission direction is different for bidirectional FD and BS FD. This is a further reason for their performance difference, besides the presence of intra-cell interference in BS FD.

The CDF of the average packet delay is shown in Fig. 17. We can observe that the delay shows approximately the same trends as the TP results. Bidirectional FD can reduce the delay when the transport protocol is UDP, while in case TCP is used, the delay increases dramatically. On the other hand, BS FD shows nearly the same results for UDP and TCP, but in this case, any of the two link directions can be improved by using FD. Finally, the RU is depicted in Fig. 18. The figure shows that bidirectional FD is able to reduce the channel occupancy in case UDP is used. However, with TCP, such type of FD requires a larger amount of TTIs to transmit the same amount of data than HD. In case of BS FD, the channel occupancy is slightly larger than with HD, due to the performance of the DL direction.

The numerical results when the traffic is asymmetric are presented in Table 2. From previous analysis, we would expect that the UL direction can always be significantly improved by the use of FD, since with HD it gets less transmission opportunities. Starting with the bidirectional FD case, we observe that simultaneous transmission and reception can always improve the system TP and delay in case UDP is used, specially the UL direction. However, when TCP is enabled, the same situation as in the symmetric traffic case is repeated. An SINR difference of 9 dB in average causes the FD system to perform worse than HD. Not even the UL, which is the lightly loaded link that gets the chance of being transmitted immediately with FD can be improved. Even though FD allows the TCP congestion window to grow faster because the TCP ACKs can be transmitted immediately, the increase in the network interference has an important impact on FD. The increase of the number of HARQ retransmission and the reduction in MCS and transmission rank compared to HD compromises the performance of FD in ultra-dense small cell scenarios. Notice that such large numbers are also dictated by the fact that the absolute delay results are very low. Moving to the BS FD case, we also observe a similar behavior as in the symmetric traffic case. The main difference is that with asymmetric traffic, we can detect an improvement of the lightly loaded link. However, the gain is rather limited. This is because the DL

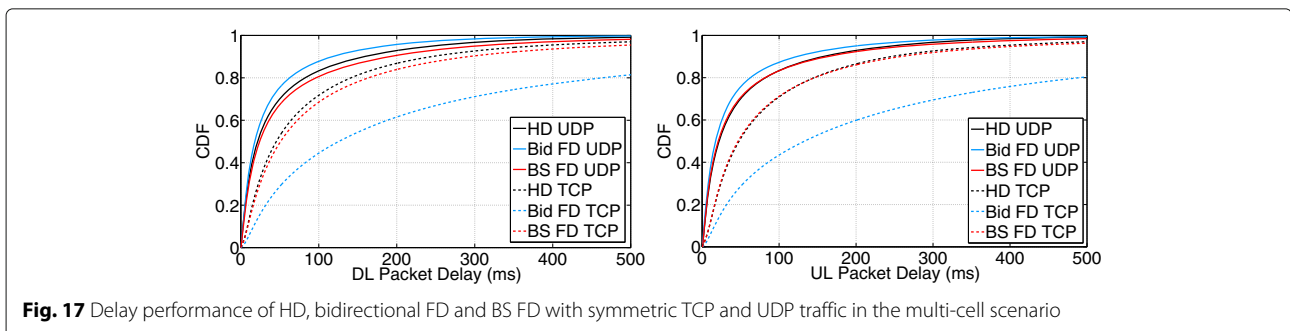
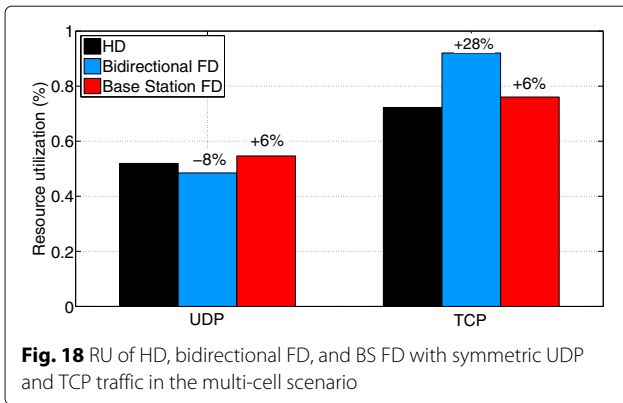


**Fig. 17** Delay performance of HD, bidirectional FD and BS FD with symmetric TCP and UDP traffic in the multi-cell scenario



direction, affected by the intra-cell interference, increases the HARQ retransmissions and thus enlarges the originally 6DL:1UL asymmetry. Consequently, the DL is even more over-prioritized, thus affecting indirectly the UL performance.

From this intensive analysis of the FD performance in 5G ultra-dense small cell networks, we can conclude that in interference-limited scenarios, the use of FD is not always beneficial. The fact that simultaneous transmission and reception doubles the amount of interfering streams has a negative impact on the system performance. However, a combination of FD and HD transmission modes may provide the optimal system performance. Finally, results indicate that FD shows potential in asymmetric traffic applications where the lightly loaded link needs to be enhanced.

### 6 Future work

Future research could analyze how non-ideal self-interference cancellation and larger traffic asymmetries between the UL and DL directions impact the results presented in this work, since they provide an upper bound of the achievable FD gain. Furthermore, the use of full duplex could be studied in the context of macro-cell scenarios, where on the other side, the self-interference is much higher in macro BS and can jeopardize the performance. In this case, MAC schemes that take into account the distance among the nodes and

power control can be designed to get the most benefit from the usage of full-duplex communication. Another interesting scenario could be the one where not all the user equipments are full duplex capable, i.e., a combination of bidirectional full duplex and base station only full duplex. Finally, the potential of simultaneous transmission and reception to provide fast discovery on the context of device-to-device (D2D) communication can be studied.

The findings presented in this paper could be applied to design a hybrid HD/FD scheduling mechanism that obtains the maximum benefit from both types of communication.

### 7 Conclusions

This work analyzes the potential of full-duplex technology in enhancing the throughput and delay of 5G ultra-dense small cell networks. The self-interference cancellation capabilities are investigated using our own developed test bed. The carried experiment proves that up to ~100 dB of isolation between the transmitting and the receiving antennas placed in the same device are currently achievable, according to the used setup. Then, the potential of full-duplex communication is studied via detailed system level simulations. Results show that achieving the theoretical double throughput gain that FD promises can only be achieved under specific assumptions, namely ideal self-interference cancellation, isolated cells, and full buffer traffic model. However, the promised gain is reduced when realistic assumptions, such as traffic constraints and the inter-cell interference, are considered. Simulations prove that when the traffic profile allows the system to use full-duplex communication, the increased interference caused by simultaneous transmission and reception becomes the main limiting factor in achieving the theoretical FD throughput gain. In case where only the base station is full duplex capable, the intra-cell interference has a significant impact on the system performance.

This work proves that full-duplex communication is able to accelerate the dynamics of TCP and mitigate the drawbacks introduced by such protocol. Furthermore,

**Table 2** TP gain and delay reduction of bidirectional FD and BS FD over HD with asymmetric TCP and UDP traffic in the multi-cell scenario

Communication type	Traffic	DL TP (%)	UL TP (%)	DL delay (%)	UL delay (%)
Bidirectional FD	UDP	+4	+18	-8	-35
	TCP	-64	-44	+548	+155
BS FD	UDP	-2	+14	+11	-18
	TCP	-12	+16	+30	-21

results of such technology has a compelling potential for applications with asymmetric traffic where the lightly loaded link can benefit in terms of throughput and delay.

**Competing interests**

The authors declare that they have no competing interests.

Received: 29 June 2016 Accepted: 26 November 2016

Published online: 13 December 2016

**References**

1. Cisco, Cisco Visual Networking Index: Global Mobile Data Traffic Forecast Update, 2015-2020 (2016)
2. P Mogensen, et al, in *2014 IEEE 79th Vehicular Technology Conference (VTC Spring)*. Centimeter-wave concept for 5g ultra-dense small cells, (Seoul, 2014), pp. 1–6. doi:10.1109/VTCspring.2014.7023157
3. JI Choi, et al, in *Proceedings of the 16th Annual International Conference on Mobile Computing and Networking (Mobicom)*. Achieving single channel, full duplex wireless communication (ACM, New York, 2010), pp. 1–12. doi:10.1145/1859995.1859997
4. E Aryafar, et al, in *Proceedings of the 18th Annual International Conference on Mobile Computing and Networking (Mobicom)*. MIDU: enabling MIMO full duplex (ACM, New York, 2012), pp. 257–268. doi:10.1145/2348543.2348576
5. S Hong, et al, Applications of self-interference cancellation in 5G and beyond. *IEEE Commun. Mag.* **52**(2), 114–121 (2014). doi:10.1109/MCOM.2014.6736751
6. M Heino, et al, Recent advances in antenna design and interference cancellation algorithms for in-band full duplex relays. *IEEE Commun. Mag.* **53**(5), 91–101 (2015). doi:10.1109/MCOM.2015.7105647
7. E Everett, A Sahai, A Sabharwal, Passive self-interference suppression for full-duplex infrastructure nodes. *IEEE Trans. Wireless Commun.* **13**(2), 680–694 (2014). doi:10.1109/TWC.2013.010214.130226
8. KM Thilina, et al, Medium access control design for full duplex wireless systems: challenges and approaches. *IEEE Commun. Mag.* **53**(5), 112–120 (2015). doi:10.1109/MCOM.2015.7105649
9. G Liu, FR Yu, H Ji, VCM Leung, X Li, In-band full-duplex relaying: a survey, research issues and challenges. *IEEE Commun. Surv. Tutorials.* **17**(2), 500–524 (2015). doi:10.1109/COMST.2015.2394324
10. T Riihonen, S Werner, R Wichman, EZ B., in *IEEE 10th Workshop on Signal Processing Advances in Wireless Communications*. On the feasibility of full-duplex relaying in the presence of loop interference, (Perugia, 2009), pp. 275–279. doi:10.1109/SPAWC.2009.5161790
11. D Bharadia, S Katti, in *Proceedings of the 11th USENIX Conference on Networked Systems Design and Implementation*. Full duplex MIMO radios. NSDI'14 (USENIX Association, Berkeley, 2014), pp. 359–372. <http://dl.acm.org/citation.cfm?id=2616448.2616482>
12. X Xie, X Zhang, in *Proceedings of IEEE INFOCOM*. Does full-duplex double the capacity of wireless networks?, (Toronto, 2014), pp. 253–261. doi:10.1109/INFOCOM.2014.6847946
13. BP Day, et al, in *Conference on Signals, Systems and Computers (ASILOMAR)*. Full-duplex bidirectional MIMO: achievable rates under limited dynamic range, vol. 60, (2012), pp. 3702–3713. *IEEE Transactions on Signal Processing*. doi:10.1109/ACSSC.2011.6190243
14. AC Cirik, R Wang, Y Hua, in *Conference on Signals, Systems and Computers (ASILOMAR)*. Weighted-sum-rate maximization for bi-directional full-duplex MIMO systems, vol. 63, (2015), pp. 801–815. *IEEE Transactions on Communications*. doi:10.1109/ACSSC.2013.6810575
15. NH Mahmood, et al, in *2015 IEEE 81st Vehicular Technology Conference (VTC Spring)*. On the potential of full duplex communication in 5G small cell networks, (Nanjing, 2015), pp. 1–5. doi:10.1109/VTCspring.2015.7145975
16. W Zhou, K Srinivasan, in *2014 International Conference on Signal Processing and Communications (SPCOM)*. Sim+: a simulator for full duplex communications, (Bangalore, 2014), pp. 1–6. doi:10.1109/SPCOM.2014.6983995
17. Z Tong, M Haenggi, Throughput analysis for full-duplex wireless networks with imperfect self-interference cancellation. *IEEE Trans. Commun.* **63**(11), 4490–4500 (2015). doi:10.1109/TCOMM.2015.2465903
18. M Mohammadi, HA Suraweera, I Krikidis, C Tellambura, in *IEEE International Conference on Communications (ICC)*. Full-duplex radio for uplink/downlink transmission with spatial randomness, (London, 2015), pp. 1908–1913. doi:10.1109/ICC.2015.7248604
19. R Zhang, et al, in *2015 IEEE International Conference on Communications (ICC)*. Investigation on DL and UL power control in full-duplex systems, (London, 2015), pp. 1903–1907. doi:10.1109/ICC.2015.7248603
20. S Goyal, et al, Full duplex cellular systems: will doubling interference prevent doubling capacity?. *IEEE Commun. Mag.* **53**(5), 121–127 (2015). doi:10.1109/MCOM.2015.7105650
21. H Malik, M Ghorraishi, R Tafazolli, in *Networks and Communications (EuCNC), 2015 European Conference On*. Cross-layer approach for asymmetric traffic accommodation in full-duplex wireless network, (Paris, 2015), pp. 265–269. doi:10.1109/EuCNC.2015.7194081
22. NH Mahmood, et al, in *11th International Conference on Wireless and Mobile Communications (ICWMC)*. Throughput analysis of full duplex communication with asymmetric traffic in small cell systems, (St. Julians, 2015), pp. 57–60
23. L Wang, et al, Exploiting full duplex for device-to-device communications in heterogeneous networks. *IEEE Commun. Mag.* **53**(5), 146–152 (2015). doi:10.1109/MCOM.2015.7105653
24. W John, S Tafvelin, in *2008 International Conference on Information Networking*. Heuristics to classify internet backbone traffic based on connection patterns, (GinoWan, 2008), pp. 1–5. doi:10.1109/ICOIN.2008.4472818
25. J Postel, Transmission Control Protocol. [Online]. Available: <http://www.ietf.org/rfc/rfc793.txt> (1981, updated by RFCs 1122, 3168, 6093, 6528)
26. M Allman, V Paxson, W Stevens, Congestion Control to TCP's Fast Recovery Algorithm. (1999, TCP, [Online]. Available: <http://www.ietf.org/rfc/rfc2581.txt> (obsoleted by RFC 5681, updated by RFC 3390)
27. m. Duarte, C Dick, A Sabharwal, Experiment-driven characterization of full-duplex wireless systems. *IEEE Trans Wireless Commun.* **11**(12), 4296–4307 (2012). doi:10.1109/TWC.2012.102612.111278
28. A Sahai, et al, On the impact of phase noise on active cancelation in wireless full-duplex. *IEEE Trans. Veh. Technol.* **62**(9), 4494–4510 (2013). doi:10.1109/TVT.2013.2266359
29. D Korpi, et al, in *IEEE Global Communications Conference (GLOBECOM)*. Adaptive nonlinear digital self-interference cancellation for mobile inband full-duplex radio: algorithms and RF measurements, (San Diego, 2015), pp. 1–7. doi:10.1109/GLOCOM.2015.7417188
30. L Anttila, et al, in *2014 IEEE Globecom Workshops (GC Wkshps)*. Modeling and efficient cancellation of nonlinear self-interference in MIMO full-duplex transceivers, (Austin, 2014), pp. 777–783. doi:10.1109/GLOCOMW.2014.7063527
31. 3rd Generation Partnership Project, Technical Specification Group Radio Access Network; Enhanced performance requirement for LTE User Equipment (UE) (2015). 3GPP TR 36.829, Enhanced performance requirement for LTE User Equipment (UE), Release 11
32. MG Sarret, et al, in *2014 11th International Symposium on Wireless Communications Systems (ISWCS)*. Improving link robustness in 5G ultra-dense small cells by hybrid arq, (Barcelona, 2014), pp. 491–495. doi:10.1109/ISWCS.2014.6933403
33. N Mahmood, D Catania, M Lauridsen, G Berardinelli, P Mogensen, F Tavares, K Pajukoski, *A Novel Centimeter-Wave Concept for 5G Small Cells. Opportunities in 5G Networks: A Research and Development Perspective*. CRC Press LLC, 5th April 2016. (F Hu, ed.) (CRC Press LLC, 2016), pp. 391–424
34. S Floyd, T Henderson, A Gurtov, The New Reno Modification to TCP's Fast Recovery Algorithm. (2004 [Online]. Available: <http://www.ietf.org/rfc/rfc3782.txt> (obsoleted by RFC 6582)
35. D Catania, et al, in *2015 IEEE 81st Vehicular Technology Conference (VTC Spring)*. A distributed taxation based rank adaptation scheme for 5G small cells, (Glasgow, 2015), pp. 1–5. doi:10.1109/VTCspring.2015.7145600
36. M Abramowitz, IA Stegun, *LTE for UMTS - OFDMA and SC-FDMA Based Radio Access*. (H Holma, A Toskala, eds.) (Wiley, 2009)
37. 3rd Generation Partnership Project, Further advancements for E-UTRA physical layer aspects (Release 9) (2010). 3GPP TR 36.814, Evolved Universal Terrestrial Radio Access (E-UTRA); Further advancements for E-UTRA physical layer aspects, Release 9
38. 3rd Generation Partnership Project, Technical Specification Group Radio Access Network; Evolved Universal Terrestrial Radio Access (E-UTRA) Radio Link Control (RLC) protocol specification (20016). 3GPP TS 36.322,

Evolved Universal Terrestrial Radio Access (E-UTRA); Radio Link Control (RLC) protocol specification, Release 8

39. J Postel, Internet Standard, User Datagram Protocol. 28th August 1980, RFC 768 (1980). <https://tools.ietf.org/html/rfc768>
40. Radio WWIN, WINNER II channel models (2008). Internet Standard, User Datagram Protocol, J. Postel, 28th August 1980, RFC 768. [www.cept.org/files/1050/documents/winner2%20-%20final%20report.pdf](http://www.cept.org/files/1050/documents/winner2%20-%20final%20report.pdf)

**Submit your manuscript to a SpringerOpen<sup>®</sup> journal and benefit from:**

- ▶ Convenient online submission
- ▶ Rigorous peer review
- ▶ Immediate publication on acceptance
- ▶ Open access: articles freely available online
- ▶ High visibility within the field
- ▶ Retaining the copyright to your article

---

Submit your next manuscript at ▶ [springeropen.com](http://springeropen.com)

---